

## Molecular-dynamics simulation for the dynamic-structure factor of commensurate krypton on graphite

N. D. Shrimpton and W. A. Steele

*Department of Chemistry, The Pennsylvania State University, 152 Davey Laboratory, University Park, Pennsylvania 16802*

(Received 1 March 1991)

The dynamic structure factor  $S(\mathbf{q}, \omega)$  for a commensurate layer of krypton on a model graphite surface is calculated from molecular-dynamics simulations. The simulations are carried out at a number of temperatures ranging up to 70 K to assess the thermal variation of  $S(\mathbf{q}, \omega)$ . These results are compared with a harmonic-lattice-dynamics calculation of the phonon spectra. The multiphonon content of  $S(\mathbf{q}, \omega)$  is shown to be minor at the temperatures considered. The temperature dependence of the zone-center frequency is attributed to thermal averaging of the substrate corrugation. The results are compared with previous studies of this system and with available experimental data.

### I. INTRODUCTION

Physisorbed systems have provided a fascinating source of study for the past two decades. Despite the attention that such systems have received, however, an understanding of the atomic interactions in these systems remains quantitatively incomplete. There are two types of molecular interactions present in physisorbed systems: between adsorbed gas atoms, and between the adsorbed gas atom and the substrate. The interaction between adsorbed atoms is modified from its bulk form by the substrate. While there are theories that predict the nature of this modification,<sup>1</sup> the details of these effects remain experimentally unconfirmed. More significantly, however, the lateral variation in the atom-substrate interaction, otherwise known as the substrate corrugation, is still not adequately described.

The observed phases formed in physisorbed monolayers often suggest a much higher corrugation value than is suggested by theoretical calculations.<sup>2</sup> This is especially true in the case of rare gases physisorbed on platinum.<sup>3</sup> Furthermore, there are calculations that suggest that for krypton on graphite, thermal effects can cause the effective value of the corrugation to vanish at temperatures higher than 40 K.<sup>4</sup> This is totally contrary to the observation that krypton forms a phase that remains commensurate with the graphite surface at temperatures up to 130 K.<sup>5</sup>

Experimentally, information about the interactions can be obtained from a variety of sources.<sup>6</sup> For the Kr-graphite corrugation, information has been obtained from a specific-heat study.<sup>7</sup> However, the best information about the corrugation can be obtained from inelastic-scattering studies such as that performed for the system of N<sub>2</sub> on graphite<sup>8</sup> and Kr on graphite.<sup>9</sup> Such studies can also potentially provide information about the adatom-adatom interactions as well. However, scattering studies are necessarily performed at finite temperatures and the effective interactions within the system are thermally altered. There are predictions from self-

consistent phonon calculations that this effect can be significant.<sup>4</sup> Consequently, we seek in this computer simulation study to shed some light on how inelastic-scattering information is modified by temperature, and how such information can be used to provide quantitative information on the interactions in simple physisorbed systems.

In inelastic scattering, the dynamical information obtained can be factored from the scattering cross-section information. This factored term is the dynamic-structure factor  $S(\mathbf{q}, \omega)$ : It is a function of the wave vector  $\mathbf{q}$  and energy  $\hbar\omega$  change associated with the process of scattering. If the adsorbed gas atoms are all of the same isotope and if they are all in the same nuclear spin state, the scattering is totally coherent and

$$S(\mathbf{q}, \omega) = \int e^{i\omega t} \sum_{m,n} \langle e^{i\mathbf{q}\cdot\mathbf{r}_m(0)} e^{-i\mathbf{q}\cdot\mathbf{r}_n(t)} \rangle dt, \quad (1)$$

where the  $\mathbf{r}_n$  are the positions of the adsorbed atoms. The quantity in angular brackets is known as the intermediate scattering factor  $F(\mathbf{q}, t)$  and is a statistical sampling of all possible states of the system. By factoring the terms of  $F(\mathbf{q}, t)$  into the function

$$\rho(\mathbf{q}, t) = \sum_n e^{i\mathbf{q}\cdot\mathbf{r}_n(t)} \quad (2)$$

the ensemble average is merely the autocorrelation of  $\rho(\mathbf{q}, t)$ , the spatial Fourier transform of the particle number density  $\rho(\mathbf{r}, t)$ .<sup>10</sup> Such autocorrelation information can be obtained by molecular-dynamics simulations.

It is immediately noted that a molecular-dynamics simulation is a classical calculation and quantum effects are not included. In classical calculations, autocorrelation functions are even in frequency, whereas quantum results must satisfy a detailed balance condition.<sup>11</sup> The dynamic-structure factor obtained classically can be corrected to first order in  $\hbar$  for this quantum effect by applying a factor

$$S(\mathbf{q}, \omega)_{\text{correct}} = e^{\hbar\omega\beta/2} S(\mathbf{q}, \omega)_{\text{classical}}. \quad (3)$$

Other quantum effects, such as zero point motion, will be discussed later with the results.

Particularly useful systems to study with inelastic scattering are commensurate physisorbed monolayers where the adsorbed atoms are in a regular lattice at adsorption sites of the substrate. Because of their high symmetry, the dynamics of these systems are particularly simple. The substrate interaction holds each atom at an adsorption site and prevents the monolayer from translating. Therefore, acoustic vibrational modes are absent and the minimum possible vibrational frequency, attained by the zone-center vibrational modes, depends upon the effective substrate corrugation. The vibrational frequencies of modes away from the zone center provide information to determine the interactions between adatoms.

However, because inelastic scattering involves multiple phonon events, information about the phonon modes of the system is obscured. How much of the frequency information is obscured by multiple phonon events can be calculated through the molecular-dynamics simulation. By expanding the intermediate scattering factor in terms of the adsorbed atom displacements  $\mathbf{r}_n(t) - \mathbf{R}_n$  from the averaged lattice sites  $\mathbf{R}_n$ , the one-phonon and multiple phonon content of  $S(\mathbf{q}, \omega)$  can be assessed. For a commensurate monolayer the averaged lattice sites  $\mathbf{R}_n$  are merely adsorption site centers. As shown by Glyde,<sup>10</sup> the one-phonon term is then

$$S^1(\mathbf{q}, \omega) = \int e^{i\omega t} \sum_{m,n} \langle \mathbf{q} \cdot \mathbf{r}_m(0) \mathbf{q} \cdot \mathbf{r}_n(t) \rangle e^{i\mathbf{q} \cdot (\mathbf{R}_m - \mathbf{R}_n)} dt. \quad (4)$$

While this term, identifying the one-phonon content of scattering, is clearly a quantum result, the actual correlation term can be calculated classically and its significance assessed against the classically obtained dynamic-structure factor.

In this paper we report molecular-dynamics simulations of a commensurate monolayer of krypton on graphite. In this system, the  $\sqrt{3} \times \sqrt{3}$  commensurate phase is formed that has the krypton atoms arranged in a triangular lattice, which places a krypton atom in every third adsorption site of the graphite substrate. Dynamic-structure factors are calculated for this phase at a variety of temperatures. The temperature variation of this information is analyzed and we show how this information can be used to understand the basic interactions in the system.

## II. CALCULATION

In the simulation, a circular patch 200 Å across of 1997 krypton atoms is taken. Each atom is initially placed in a commensurate  $\sqrt{3} \times \sqrt{3}$  adsorption site. A circular patch provides a different set of boundary conditions from the usual periodic ones and frees the simulation from having only a discrete set of vibrational wave vectors and also allows the significance of the free edge to be assessed.

The krypton interaction  $U(r)$  is modeled by a 6-12 pair potential

$$U(r) = 4\epsilon \left[ \left( \frac{\sigma}{r} \right)^{12} - \left( \frac{\sigma}{r} \right)^6 \right], \quad (5)$$

where  $\epsilon = 170$  K and  $\sigma = 3.60$  Å. The Kr-substrate interaction is obtained by a pair summation of the interaction of the krypton atom with each individual graphite atom in the substrate. The Kr-C atom interaction is also modeled by a 6-12 interaction with  $\epsilon = 75$  K and  $\sigma = 3.42$  Å. It is known from numerous other studies that this model yields observable properties in reasonable agreement with experiment.<sup>12</sup> Given the periodicity of the substrate, the holding potential can be described as

$$V(\mathbf{r}, z) = V_0(z) + \sum_{\mathbf{g}} V_{\mathbf{g}}(z) e^{i\mathbf{g} \cdot \mathbf{r}}, \quad (6)$$

where the summation runs over all reciprocal-lattice vectors  $\mathbf{g}$  of the substrate,  $z$  is the height of the adatom above the substrate, and  $\mathbf{r}$  is the location of the adatom along the substrate. Calculations show that the summation can be truncated after the first shell of six  $\mathbf{g}$ 's. By symmetry,  $V_{\mathbf{g}}(z)$  does not vary with the orientation of  $\mathbf{g}$  and can be factored from the summation. The resulting factor  $V_{\mathbf{g}}(z)$  is known as the corrugation of the substrate. It has been suggested by several workers that the assumption of pairwise carbon-gas interaction gives a corrugation that is too small. In particular, it is known that this corrugation prevents the monolayer from forming a commensurate phase. In order to assure that the commensurate phase is stable, the form of (6) is corrected in this work by multiplying the corrugation term by a constant factor  $s$  so that

$$V(\mathbf{r}, z) = V_0(z) + s \sum_{\mathbf{g}} V_{\mathbf{g}}(z) e^{i\mathbf{g} \cdot \mathbf{r}}. \quad (7)$$

For this work  $s$  is given the value 1.5. This is within the range suggested by Vidali and Cole,<sup>13</sup> and is large enough to ensure that a commensurate configuration is obtained.

The molecular-dynamics simulation is initialized by a constant temperature equilibration run of up to 100 ps. The dynamic-structure factors are then obtained from a constant energy run of 400 ps. The algorithm is the standard Verlet scheme as modified by Swope *et al.*<sup>14</sup> to allow the simultaneous knowledge of position and velocity. The time step is 5 fs at low temperatures and 4 fs at 70 K. At a specified times  $t$ , spaced at intervals of 0.25 ps in the simulation, the density function  $\rho(\mathbf{q}, t)$  [see Eq. (2)] is determined for a variety of wave vectors  $\mathbf{q}$ .

Given that the dynamic-structure factor  $S(\mathbf{q}, \omega)$  is just the temporal Fourier transform of the intermediate scattering function  $F(\mathbf{q}, t) = \langle \rho^*(\mathbf{q}, 0) \rho(\mathbf{q}, t) \rangle$ ,  $S(\mathbf{q}, \omega)$  can be reduced to a Weiner-Khintchine form

$$S(\mathbf{q}, \omega) = \rho(\mathbf{q}, \omega) \rho^*(\mathbf{q}, \omega), \quad (8)$$

where

$$\rho(\mathbf{q}, \omega) = \int e^{i\omega t} \rho(\mathbf{q}, t) \quad (9)$$

and normalizations have been set aside.

$S(\mathbf{q}, \omega)$  is the full scattering factor and consequently includes the  $\delta$ -function singularity at  $\omega = 0$  associated with elastic scattering. This singularity can numerically corrupt the inelastic-scattering information and it is advantageous to redefine  $S(\mathbf{q}, \omega)$  to omit the elastic information. One notes that

$$\rho(\mathbf{q}, t) = \int \rho(\mathbf{r}, t) e^{i\mathbf{q}\cdot\mathbf{r}} d\mathbf{r}, \quad (10)$$

where  $\rho(\mathbf{r}, t) = \sum_n \delta[\mathbf{r} - \mathbf{r}_n(t)]$ . By defining

$$\delta\rho(\mathbf{q}, t) = \int [\rho(\mathbf{r}, t) - \rho_0(\mathbf{r})] e^{i\mathbf{q}\cdot\mathbf{r}} d\mathbf{r} \quad (11)$$

in terms of the density fluctuation about the average density profile  $\rho_0(\mathbf{r})$ , the full dynamic structure factor can be written

$$S(\mathbf{q}, \omega) = \delta(\omega) S_0(\mathbf{k}) + \delta\rho(\mathbf{q}, \omega) \delta\rho^*(\mathbf{q}, \omega), \quad (12)$$

where  $S_0(\mathbf{k})$  is the structure factor,  $\delta\rho(\mathbf{q}, \omega)$  is the temporal Fourier transform of  $\delta\rho(\mathbf{q}, t)$ , and everything has been suitably normalized. The inelastic part of  $S(\mathbf{q}, \omega)$ , which from now on will be called  $S(\mathbf{q}, \omega)$ , is merely  $\delta\rho(\mathbf{q}, \omega) \delta\rho^*(\mathbf{q}, \omega)$ .

Rather than storing all the time-dependent information and performing Fast Fourier transforms (FFT's) at the end of the simulation, it is sometimes convenient to perform temporal Fourier transforms during the course of the run. However,  $\delta\rho(\mathbf{q}, \omega)$  requires knowledge of the final averaged density profile  $\rho_0(\mathbf{r})$  at each time step to subtract the elastic information. (Performing the subtraction at the end of the run is not useful as both terms involve the  $\omega$  elastic singularity and the numerical inaccuracies associated with this singularity are not avoided.)

But considering that

$$g(\mathbf{q}, t) = \frac{\partial}{\partial t} \delta\rho(\mathbf{q}, t) = \sum_n i\mathbf{v}_n(t) \cdot \mathbf{q} e^{i\mathbf{q}\cdot\mathbf{r}_n(t)} \quad (13)$$

can be obtained at each time step, a temporal transform can be performed over the course of the run to get  $g(\mathbf{q}, \omega)$ . Then  $\delta\rho(\mathbf{q}, \omega) = (1/\omega)g(\mathbf{q}, \omega)$  and

$$S(\mathbf{q}, \omega) = \left| \frac{g(\mathbf{q}, \omega)}{\omega} \right|^2. \quad (14)$$

This also has the added advantage that the periodicity of  $2\pi/\Delta t$  in  $\omega$  implicit with a discrete temporal sampling of interval  $\Delta t$  occurs in the quantity  $g(\mathbf{q}, \omega)$ , and this effect is diminished for the quantity  $\delta\rho(\mathbf{q}, \omega)$ .

Likewise, the one-phonon contribution  $S^1(\mathbf{q}, \omega)$  to the scattering, which is obtained from (4), can be calculated from

$$g'(\mathbf{q}, t) = \sum_n i\mathbf{v}_n(t) \cdot \mathbf{q} e^{i\mathbf{q}\cdot\mathbf{R}_n} \quad (15)$$

so that

$$S^1(\mathbf{q}, \omega) = \left| \frac{g'(\mathbf{q}, \omega)}{\omega} \right|^2. \quad (16)$$

By comparing (14) and (16), the effect of multiple phonon events on the dynamic-structure factor can be assessed.

### III. RESULTS

The dynamic-structure factors are obtained at a variety of wave vectors for several runs of 400 ps at a variety of temperatures. The positions of the wave vectors in the Brillouin zone are indicated in Fig. 1. The dynamic-

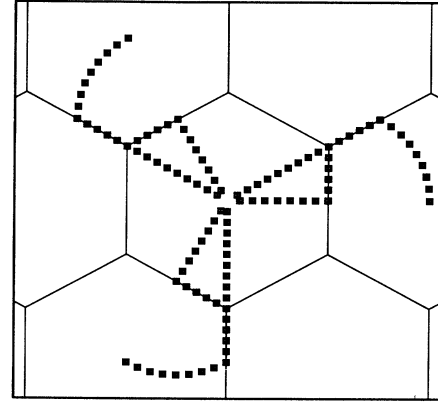


FIG. 1. The wave vector points at which the dynamic-structure factor is calculated are shown. The solid lines indicate the edge of the Brillouin zones. The center of each Brillouin zone is known as the  $\Gamma$  point. The point at the middle of a Brillouin-zone edge is the  $M$  point, and the corner of the Brillouin zone is the  $K$  point.

structure factor only contains information about motion that is parallel to the direction of the wave vector. Consequently, the frequency dependence of  $S(\mathbf{q}, \omega)$  for wave vectors within the first Brillouin zone will reflect vibrational modes that are predominantly longitudinal. In the surrounding, or secondary, Brillouin zones, the direction of the modes at each wave vector will be with respect to the secondary Brillouin-zone centers. Consequently, along the arcs of wave vectors ( $\Gamma$  to  $M$ ) shown in Fig. 1, the wave vector will be perpendicular to the direction of the secondary zone center: Information obtained at these points will contain information about vibrational modes with large transverse components. The paths from  $K$  to  $M$  in the secondary Brillouin zones do not provide this restriction to longitudinal or transverse content, except at the  $M$  point. However, because the longitudinal and transverse modes have the same frequencies at  $K$ , information along this path does provide information about the transverse  $K$  to  $M$  branch. By taking information at the three symmetrically redundant  $\mathbf{q}$  vectors, the statistics for each wave-vector point is tripled for each run.

Information about the effect of the free edge of the simulated Kr film is obtained by calculating  $S(\mathbf{q}, \omega)$  with various cutoffs imposed. The summation over adatoms in (13) is performed for all atoms, for all atoms within a central 80-Å circle, and for all atoms with each contribution given a weight factor. The weight factors had a Gaussian profile with a peak at the center. Two profiles were chosen, one that diminished by half at a radius of 25 Å and one that diminished by half at a radius of 66 Å. The Gaussian weight factors, while restricting  $S(\mathbf{q}, \omega)$  from having information about the edge, also provide a smoothing of the structure factor by including a Gaussian convolution in  $\mathbf{q}$  that ranged in half-width from 0.04 to 0.1 Å<sup>-1</sup>. The dynamic-structure factors appeared identical within the general statistical variation of each run regardless of whether a Gaussian weight or an 80-Å

cutoff was used. Differences did occur between these structure factors and those calculated without any cutoff. Subpeaks in frequency were noted in many of the dynamic-structure factors, however the weakness of the peaks and the general statistical variation of each run made the identification of such things as Rayleigh modes impossible.

The frequency variation of  $S(\mathbf{q}, \omega)$  at 40 K for zone-center modes and for longitudinal and transverse  $M$  modes is shown in Fig. 2. The amplitude of  $S(\mathbf{q}, \omega)$  is arbitrary. Single-phonon information is also calculated from (16) and is indistinguishable from that obtained from (14). Consequently these dynamic-structure factors provide almost exclusively single-phonon information. Phonon lifetimes can be estimated from the width at half height, which is roughly  $1 \times 10^{11}$  rad/sec for zone-center

modes and transverse zone-edge modes, and  $5 \times 10^{11}$  rad/sec for the longitudinal zone-edge modes. This would give phonon half-lives for several picoseconds at 40 K. The relatively long half-life of the modes points out a problem with trying to obtain amplitude information from such calculations of  $S(\mathbf{q}, \omega)$ . At every instant in time, every phonon mode is not necessarily present at the amplitude appropriate to its ensemble average. Only at time scales much longer than the phonon lifetimes will every mode on average be represented appropriately. Given that constraints of practicality limit the runs to 400 ps, it is not possible to establish full ensemble statistics through these simulations. This does not imply, however, that  $S(\mathbf{q}, \omega)$  information obtained is without value. The peaks of  $S(\mathbf{q}, \omega)$  do occur at frequencies appropriate to the phonon vibrational modes, it is only that

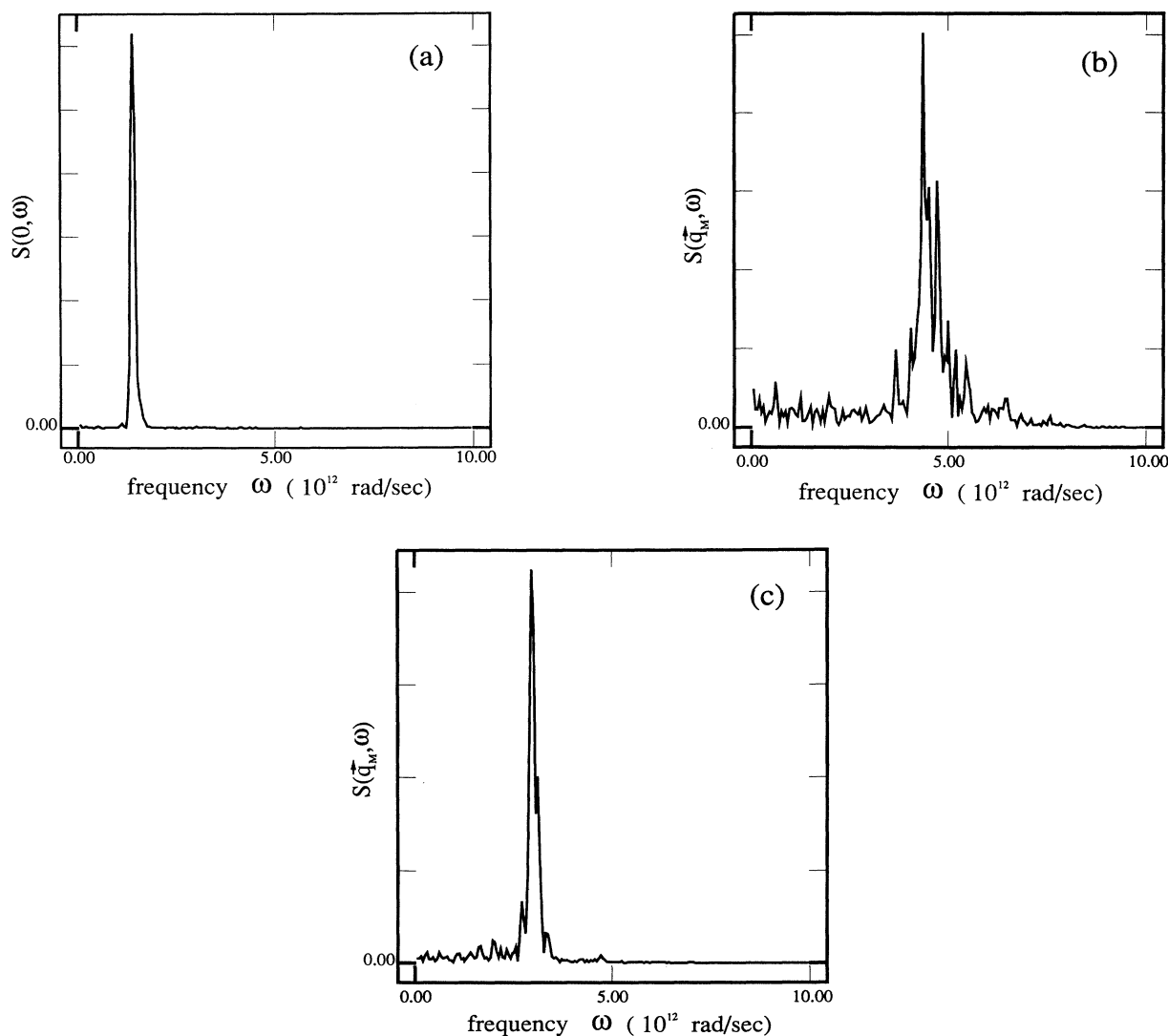


FIG. 2. The dynamic-structure factor evaluated at zone center is shown in (a). The dynamic-structure factor evaluated at the  $M$  point of the central Brillouin zone is shown in (b); this gives information about the longitudinal motion. The dynamic-structure factor evaluated at the  $M$  point at the connecting edge of the surrounding Brillouin zones is shown in (c); this gives information about the transverse motion.

the peak shapes are distorted from true ensemble forms. The peak widths in Fig. 2 represent a resolution inaccuracy in the peak frequency as much as they imply lifetime information. Longitudinal modes have the broadest peaks and for wave vectors along the zone edges the width ranges roughly from  $4 \times 10^{10}$  rad/sec at 10 K to  $5 \times 10^{11}$  rad/sec at 40 K.

A plot of the peak frequencies at each wave vector for temperatures of 10, 20, and 40 K is shown in Fig. 3. The phonon mode frequencies obtained from a standard lattice-dynamics normal mode calculation are also shown. It is clear that commensurate krypton has normal mode dynamics over this temperature range, although the frequency values shift with temperature.

Information about the interactions in the system can be extracted from these dispersion curves. From the normal mode calculation,

$$\omega^2(\mathbf{q}) = \omega_0^2 + \Omega^2(\mathbf{q}), \quad (17)$$

where  $\Omega(\mathbf{q})$  is the dispersion relationship associated with the free floating monolayer and is dependent entirely on the interactions between the adsorbed atoms.  $\omega_0$  is obtained from the in-plane diagonal elements of the tensor  $\nabla \nabla V(\mathbf{r}, z)$  and depends solely on the adatom-substrate interaction. Because of the symmetry of  $V(\mathbf{r}, z)$  about the adsorption sites, the diagonal elements are merely  $3g^2 V_g$ , where  $g$  is the length of the first-shell reciprocal-lattice vector of the substrate, and  $V_g$  is the value of  $V_g(z)$  evaluated at the adsorption site minimum of energy. Thus,

$$\omega_0 = g \sqrt{3V_g/m}. \quad (18)$$

Because  $\Omega(\mathbf{q})=0$  when  $\mathbf{q}=0$ , a value can be found for the band gap  $\omega_0$  from zone-center scattering information. Scattering information away from the zone center then provides information about the interactions between the adatoms.

Peaks in  $S(\mathbf{q}=0, \omega)$  are extremely well defined even for

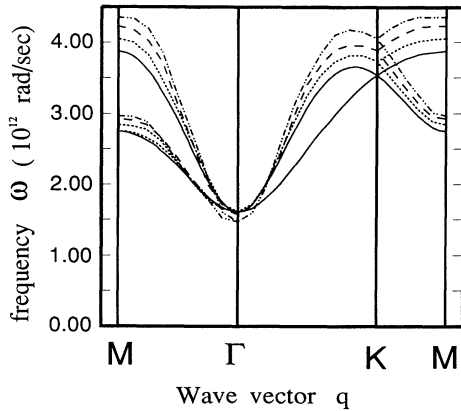


FIG. 3. This figure gives the peak frequencies of the dynamic-structure factors at various wave vectors at the temperatures of 10 K (short-dashed line), 20 K (long-dashed line), and 40 K (dashed-double-dotted line). Also shown (solid line) are the phonon modes evaluated from a harmonic-lattice-dynamics calculation.

temperatures up to 70 K. These are calculated for a range of temperatures and the frequency of the peak at each temperature is shown in Table I. The frequency at 70 K with  $s=1.5$  can be compared with the preliminary results obtained by Lauter *et al.*<sup>9</sup> At this temperature they find a band-gap frequency  $f_0=0.2$  THz, or equivalently  $\omega_0=1.26 \times 10^{12}$  rad/sec, which agrees well with our result.

Also included in Table I are results from runs where the substrate corrugation factor is increased from 1.5 to 2.0. In both cases, it is interesting to note that the frequency first increases with temperature before it decreases. To understand this effect it is useful to consider the thermal average for  $V_g$ ,  $\langle V_g(z)e^{ig \cdot \mathbf{r}} \rangle$ . That the effective corrugation value should reflect such a thermal averaging was first suggested by Villain and Gordon.<sup>15</sup> This is also suggested by self-consistent phonon calculations.<sup>4,16</sup>

Because the in-plane modes and out-of-plane modes are basically decoupled, this average is split so that

$$V_g = \langle V_g(z) \rangle \langle e^{ig \cdot \mathbf{r}} \rangle. \quad (19)$$

These two thermal averages have been calculated over the course of the simulations and are shown in Table II along with the value  $V_g$  obtained from (19) and the value  $\omega_0$  obtained from (18). The calculated values of  $\omega_0$  in Table II closely match the band-gap frequencies shown in Table I, indicating that the motion of the adatoms reflects an averaging of the effective potentials.

At higher temperatures where the classical assumption is less significant, the temperature variation of  $\langle e^{ig \cdot \mathbf{r}} \rangle$  can be compared to existing self-consistent phonon results. Close agreement is found with the results of Schobinger and Koch.<sup>16</sup> Expressed in their terminology, our calculation was performed with an  $\omega_0^2=0.58$ , and identical adatom interaction potentials. At 70 K we find  $\langle e^{ig \cdot \mathbf{r}} \rangle$  is decreased to 0.64, a value that is slightly less than can be extrapolated from their results.

From the values given in Table II at low temperatures, it is clear that the initial increase with temperature of  $\omega_0$  is due to the temperature variation of  $\langle V_g(z) \rangle$ . The out-of-plane motion of the adatoms is governed primarily by  $V_0(z)$  in (7) and at low temperatures it can be considered harmonic. Because  $V_g(z)$  increases more rapidly towards the substrate than it decreases away from the substrate, thermal vibration of the atoms about the potential minima will on average increase the effective value of  $V_g(z)$ .

TABLE I. Zone-center frequencies.

$T$ (K)	$\omega_0(10^{12}$ rad/sec)	
	$s=1.5$	$s=2.0$
0	0.61	1.86
5		2.06
10	1.63	2.03
20	1.60	
40	1.43	1.80
50	1.34	1.70
70	1.28	

TABLE II. Contributions to the thermal average of the substrate corrugation for  $s = 1.5$ . The effective frequency  $\omega_0$  is also listed.

$T$ (K)	$\langle V_g(z) \rangle$ (K)	$\langle e^{i\mathbf{g}\cdot\mathbf{r}} \rangle$	$\omega_0$ ( $10^{12}$ rad/sec)
0	10.04	1.0	1.61
10	10.97	0.91	1.61
20	10.87	0.87	1.57
30	10.72	0.82	1.51
40	10.63	0.79	1.47
50	10.47	0.74	1.42
70	10.19	0.64	1.30

Such an effect has also been found in self-consistent phonon calculation of hydrogen on graphite.<sup>17</sup> At higher temperatures, however, the average height of the atoms has moved from the minimum of 3.36 Å above the substrate to 3.40 Å at 70 K. This decreases the value of  $\langle V_g(z) \rangle$ .

It is interesting to note that  $\langle e^{i\mathbf{g}\cdot\mathbf{r}} \rangle$  is related to the static structure factor measured at wave vector  $\mathbf{g}$ . Its variation with temperature is given simply by the Debye-Waller factor. Unfortunately its value for the monolayer cannot be measured by diffraction experiments as information at this point is obscured by scattering from the substrate. Information can be obtained, however, for  $\langle e^{i\mathbf{q}\cdot\mathbf{r}} \rangle$  for  $\mathbf{q}$  corresponding to the zone centers shown in Fig. 1. If the vibrations correspond to pure normal modes, then

$$\langle e^{i\mathbf{g}\cdot\mathbf{r}} \rangle = e^{-\mathbf{g}\cdot\langle(\mathbf{r}-\mathbf{R})^2\rangle\cdot\mathbf{g}} \quad (20)$$

and

$$\langle e^{i\mathbf{q}\cdot\mathbf{r}} \rangle = e^{-\mathbf{q}\cdot\langle(\mathbf{r}-\mathbf{R})^2\rangle\cdot\mathbf{q}} \quad (21)$$

where  $\mathbf{R}$  is the adsorption site center. This result is true for both the classical and quantum-mechanical harmonic system.<sup>18</sup> Because  $\mathbf{q}$  is a reciprocal-lattice vector of the  $\sqrt{3}\times\sqrt{3}$  sublattice of adsorption sites, it has a length  $1/\sqrt{3}$  of  $\mathbf{g}$  and thus  $\langle e^{i\mathbf{q}\cdot\mathbf{r}} \rangle$  should be the cube of  $\langle e^{i\mathbf{g}\cdot\mathbf{r}} \rangle$ . These two values have been calculated from the simulations and are plotted in Fig. 4. In all cases, the cubic relationship is observed, indicating that the measured zone-center information  $\langle e^{i\mathbf{q}\cdot\mathbf{r}} \rangle$  can be applied to evaluate  $\langle e^{i\mathbf{g}\cdot\mathbf{r}} \rangle$ . Consequently the reduction in the effective corrugation due to in-plane vibrations can be determined.

Also interesting is the fact that the logarithmic plots in Fig. 4 are not exponential in  $T$ . This could be expected at low temperatures because classically the mean-square displacement of the adatoms should increase linearly with temperature. However, the mean-square amplitudes also depend inversely on the frequency of the modes. Because of the rapid variation of  $\langle V_g(z) \rangle$  at low temperature, the frequency of any given mode will vary with temperature, and the plots should not be exponential.

Dispersion curve information away from the zone centers depends on  $\Omega(\mathbf{q})$  of (17). The  $\Omega(\mathbf{q})$  values are obtained from the eigenvalues of the tensor

$$\sum_{\mathbf{r}} (1 - \cos\mathbf{q}\cdot\mathbf{r}) \nabla\nabla V(\mathbf{r}), \quad (22)$$

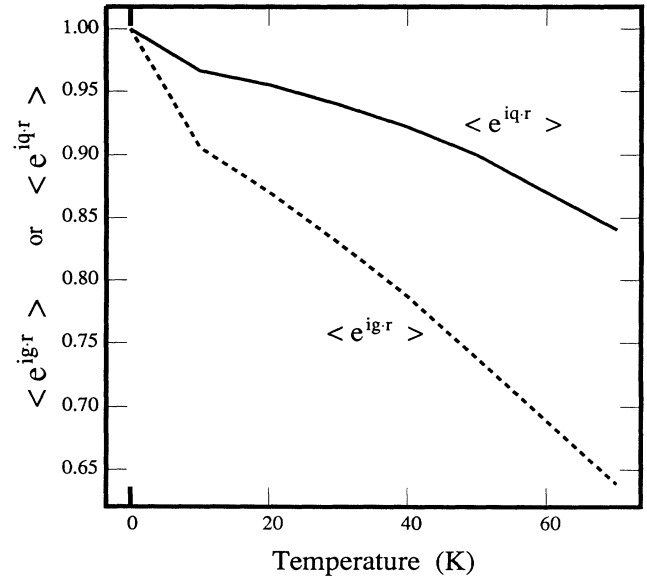


FIG. 4. This figure shows a plot of  $\langle e^{i\mathbf{q}\cdot\mathbf{r}} \rangle$  and  $\langle e^{i\mathbf{g}\cdot\mathbf{r}} \rangle$  as a function of temperature.

where the summation proceeds over the adsorption site positions, the double gradient terms of the adatom potential being the force constants of motion. With analogy to self-consistent phonon calculations, thermal averages of the force constants were evaluated at 20 and 40 K. Eigenvalues were obtained from these averaged force constants and normal mode frequencies obtained for wave vectors at the  $M$  point. While the transverse mode frequencies are close to those given in Fig. 3, the longitudinal mode frequencies are calculated to be  $4.38 \times 10^{12}$  and  $4.84 \times 10^{12}$  rad/sec at 20 and 40 K, respectively. These values can be contrasted with  $4.23 \times 10^{12}$  and  $4.35 \times 10^{12}$  rad/sec shown in Fig. 3. It is clear that the average force constants overestimate the measured frequency.

It should be remembered, however, that the normal mode calculation requires a harmonic approximation to the interaction potential. As shown by Hakim and Glyde in self-consistent phonon calculations, anharmonic terms in the effective Hamiltonian not only introduce a finite lifetime to the normal modes, they also reduce the frequency from that predicted from a harmonic Hamiltonian. Although not done in this case, it is anticipated that with the inclusion of thermally averaged anharmonic information, the calculated frequencies will match those shown in Fig. 3. This points out a limitation of using inelastic-scattering information. Such information does not necessarily give directly the effective harmonic force constants: Shifts in frequency associated with anharmonic terms in the effective Hamiltonian must also be accounted for. Consequently, for a proper evaluation of adatom interaction potentials from inelastic-scattering experiments, the only available tests may be self-consistent phonon calculations or molecular-dynamics simulations. The only remaining question then concerns the validity of classical simulations to evaluate phonon

information that may be have large quantum effects.

Again resorting to self-consistent phonon calculations, the main quantity that governs the thermal influence on the effective interactions are mean-squared mode amplitudes. Given that the motions are sufficiently harmonic, Ehrenfest theorems<sup>19</sup> will ensure that the motions of the adatom centers follow the same trajectories whether or not quantum effects are considered. What will be significant is the quantum smearing of the adatom about its central position. This will become most important at low temperatures. With quantum effects the mean-squared displacement associated with any given mode will have a temperature variation of  $(2/\hbar\omega)\coth(\hbar\omega/2k_B T)$ . Classically, however, the temperature variation will merely be  $k_B T$ . The ratio of these two values will give an indication of how significant quantum effects are. For the case of krypton on graphite, the mode frequencies range from  $2 \times 10^{12}$  rad/sec to  $4 \times 10^{12}$  rad/sec. This gives at 40 K ratios of 1.01 and 1.04, respectively. At 70 K these ratios become 1.003 and 1.01. Given that physisorption interactions are presently not known to even 4% accuracy, classical molecular-dynamics simulations together with inelastic-scattering information can provide a good test of proposed interaction potentials.

#### IV. CONCLUSION

We have presented in this paper results that show how temperature influences the dynamics of a commensurate

krypton monolayer on graphite. From comparison with experiment,<sup>9</sup> we find that the substrate potential is well described by (7) with  $s$  slightly less than 1.5. The dynamic structure is dominated by one-phonon events. The vibrational motion can be described in terms of normal modes with frequencies that are shifted and broadened by temperature. The shift of the zone-center frequency determines the temperature influence on the effective value of the substrate corrugation. The effective corrugation of the substrate first increases and then decreases with temperature. Its value results from a thermal average of the substrate potential that acts on the adsorbed atoms. This value does not decrease to zero, as suggested by Hakim and Glyde,<sup>4</sup> rather its decrease is less dramatic, as predicted by Schobinger and Koch.<sup>16</sup> Temperature also modifies the effective interactions between the adatoms. Anharmonic effects, however, preclude the frequency-shift information being directly related to the effective force constants of interaction.

#### ACKNOWLEDGMENTS

We are thankful to Toufic Hakim for providing me with a copy of his Ph.D. thesis from which many of the details of self-consistent phonon calculations become clear. We would also like to thank H. Taub for useful discussions. This work is supported by Grant No. DMR-8718771 from the Division of Materials Research of the NSF.

- 
- <sup>1</sup>O. Sinanoglu and K. S. Pitzer, *J. Chem. Phys.* **32**, 1279 (1960); A. D. McLachlan, *Surf. Sci.* **7**, 381 (1964).
- <sup>2</sup>L. W. Bruch, in *Phase Transitions in Surface Films*, edited by H. Taub, G. Torzo, H. J. Lauter, and S. C. Fain Jr. (Plenum, New York, 1991).
- <sup>3</sup>K. Kern, R. David, P. Zeppenfeld, and G. Comsa, *Surf. Sci.* **195**, 353 (1988).
- <sup>4</sup>T. M. Hakim, H. R. Glyde, and S. T. Chui, *Phys. Rev. B* **37**, 974 (1988).
- <sup>5</sup>E. D. Specht, A. Mak, C. Peters, M. Sutton, R. J. Birgeneau, K. L. D'Amico, D. E. Moncton, S. E. Nagler, and P. M. Horn, *Z. Phys. B* **69**, 347 (1987).
- <sup>6</sup>N. D. Shrimpton, M. W. Cole, and W. A. Steele, in *Surface Properties of Layered Materials*, edited by G. Benedek (Kluwer Academic, The Netherlands, 1991).
- <sup>7</sup>T. Shirakami, A. Inaba, and H. Chihara, *Thermochim. Acta* **163**, 233 (1990).
- <sup>8</sup>F. Y. Hansen, V. L. P. Frank, H. Taub, L. W. Bruch, H. J. Lauter, and J. R. Dennison, *Phys. Rev. Lett.* **64**, 764 (1990).
- <sup>9</sup>H. J. Lauter, V. L. P. Frank, H. Taub, and P. Leiderer, *Physica B+C* **165-166B**, 611 (1990); and H. Taub (private communication).
- <sup>10</sup>H. R. Glyde, *Can. J. Phys.* **52**, 2281 (1974).
- <sup>11</sup>M. P. Allen and D. J. Tildesley, *Computer Simulations of Liquids* (Oxford University Press, Oxford, 1987), p. 67.
- <sup>12</sup>W. A. Steele, *Surf. Sci.* **36**, 317 (1973).
- <sup>13</sup>G. Vidali and M. W. Cole, *Phys. Rev. B* **29**, 6736 (1984).
- <sup>14</sup>W. C. Swope, H. C. Andersen, P. H. Berens, and K. R. Wilson, *J. Chem. Phys.* **76**, 637 (1982).
- <sup>15</sup>J. Villian and M. B. Gordon, *Surf. Sci.* **125**, 1 (1983).
- <sup>16</sup>M. Schobinger and S. W. Koch, *Z. Phys. B* **53**, 233 (1983).
- <sup>17</sup>A. D. Novaco, *Phys. Rev. Lett.* **60**, 2058 (1988).
- <sup>18</sup>A. A. Maradudin, E. W. Montroll, G. H. Weiss, and I. P. Ipatova, *Theory of Lattice Dynamics in the Harmonic Approximation* (Academic, New York, 1971), p. 306.
- <sup>19</sup>See, for example, A. Messiah, *Quantum Mechanics* (North-Holland, Amsterdam, 1961).